Structural variation of forest edges across Europe

Camille Meeussen[a], Sanne Govaert[a], Thomas Vanneste[a], Kim Calders[b], Kurt Bollmann[c], Jörg Brunet[d], Sara A. O. Cousins[e], Martin Diekmann[f], Bente J. Graae[g], Per-Ola Hedwall[d], Sruthi M. Krishna Moorthy[b], Giovanni Iacopetti[h], Jonathan Lenoir[i], Sigrid Lindmo[g], Anna Orczewska[j], Quentin Ponette[k], Jan Plue[e], Federico Selvi[h], Fabien Spicher[i], Matteo Tolosano[a,l], Hans Verbeeck[b], Kris Verheyen[a], Pieter Vangansbeke[a] and Pieter De Frenne[a]

[a]Forest and Nature Lab, Department of Environment, Faculty of Bioscience Engineering, Ghent University, Geraardsbergsesteenweg 267, 9090 Melle-Gontrode, Belgium

[b]CAVElab – Computational and Applied Vegetation Ecology, Department of Environment, Faculty of Bioscience Engineering, Ghent University, Coupure Links 653, 9000 Ghent, Belgium

[c]Swiss Federal Institute for Forest, Snow and Landscape Research WSL, Zürcherstrasse 111, 8903 Birmensdorf, Switzerland

[d]Southern Swedish Forest Research Centre, Swedish University of Agricultural Sciences, Box 49, 230 53 Alnarp, Sweden

[e]Biogeography and Geomatics, Department of Physical Geography, Stockholm University, Svante Arrhenius väg 8, 106 91 Stockholm, Sweden

[f]Vegetation Ecology and Conservation Biology, Institute of Ecology, FB2, University of Bremen, Leobener Str. 5, 28359 Bremen, Germany

[g]Department of Biology, Norwegian University of Science and Technology, Høgskoleringen 5, 7491 Trondheim, Norway

[h]Department of Agriculture, Food, Environment and Forestry, University of Florence, P. le Cascine 28, 50144 Florence, Italy

24   [i]UR « Ecologie et Dynamique des Systèmes Anthropisés » (EDYSAN, UMR 7058 CNRS-UPJV),

25   Jules Verne University of Picardie, 1 Rue des Louvels, 80037 Amiens, France

26   [j]Department of Ecology, Faculty of Biology and Environmental Protection, University of Silesia,

27   Bankowa 9, 40-007 Katowice, Poland

28   [k]Earth and Life Institute, Université catholique de Louvain, Croix de Sud 2, 1348 Louvain-la-Neuve,

29   Belgium

30   [l]Stream Biofilm and Ecosystem Research Laboratory, School of Architecture, Civil and

31   Environmental Engineering, École Polytechnique Féderale de Lausanne, Bâtiment GR A1 445

32   (Station 2), 1015 Lausanne, Switzerland

33

34   **Corresponding author**

35   camille.meeussen@ugent.be

Abstract

Forest edges are interfaces between forest interiors and adjacent land cover types. They are important elements in the landscape with almost 20 % of the global forest area located within 100 m of the edge. Edges are structurally different from forest interiors, which results in unique edge influences on microclimate, functioning and biodiversity. These edge influences have been studied for multiple decades, yet there is only limited information available on how forest edge structure varies at the continental scale, and which factors drive this potential structural diversity. Here we quantified the structural variation along 45 edge-to-interior transects situated along latitudinal, elevational and management gradients across Europe. We combined state-of-the-art terrestrial laser scanning and conventional forest inventory techniques to investigate how the forest edge structure (e.g. plant area index, stem density, canopy height and foliage height diversity) varies and which factors affect this forest edge structural variability. Macroclimate, management, distance to the forest edge and tree community composition all influenced the forest edge structural variability and interestingly we detected interactive effects of our predictors as well. We found more abrupt edge-to-interior gradients (i.e. steeper slopes) in the plant area index in regularly thinned forests. In addition, latitude, mean annual temperature and humidity all affected edge-to-interior gradients in stem density. We also detected a simultaneous impact of both humidity and management, and humidity and distance to the forest edge, on the canopy height and foliage height diversity. These results contribute to our understanding of how environmental conditions and management shape the forest edge structure. Our findings stress the need for site-specific recommendations on forest edge management instead of generalized recommendations as the macroclimate substantially influences the forest edge structure. Only then, the forest edge microclimate, functioning and biodiversity can be conserved at a local scale.

1. Introduction

The interface between forest and adjacent land is gaining research relevance as it represents a substantial area; almost 20 % of the global forested area is positioned within 100 m of a forest edge (Haddad et al., 2015). The total surface area of forest edges continues to increase as forests are becoming more and more fragmented (Riitters et al., 2016; Taubert et al., 2018). According to Riitters et al. (2016), the loss of forest interiors is at least two times higher than the net loss of forest area, which results in an accumulating number of forest edges.

Forest edges help to preserve the biodiversity in the forest interior from the adverse conditions that predominate outside forest interiors and provide suitable habitat conditions for a variety of both forest specialists and generalist species (Honnay et al., 2002; Melin et al., 2018; Wermelinger et al., 2007; Govaert et al.,2019). Secondly, in addition to biodiversity, also carbon, nutrient and water cycling are altered inside forest edges (Schmidt et al., 2017). In comparison with forest interiors, forest edges are characterized by higher levels of atmospheric nitrogen deposition (Weathers et al., 2001; De Schrijver et al., 2007; Remy et al., 2016) and higher influx of herbicides and fertilizers from adjacent arable lands (Correll, 1991; Kleijn and Snoeijing, 1997). A third important characteristic of forest edges is that their microclimate is different from the forest interior (Young and Mitchell, 1994; Chen et al., 1995; Saunders et al., 1999; Schmidt et al., 2019). Forest microclimates are increasingly considered in climate-change research and imperative for the conservation of shade-tolerant forest specialists (Lenoir et al., 2017; De Frenne et al., 2019; Zellweger et al., 2019b).

Forest edges are not similar everywhere but differ in their structure, composition and functioning. Together with edge history, orientation, climate and management (Matlack, 1994; Strayer et al., 2003; Esseen et al., 2016), the adjacent, often intensive, land-use management practices will strongly impact the forest edge structure and composition. Species composition itself could further shape the edge structure as trees differ in their architecture and ability to react to the increased light availability near an edge (Mourelle et al., 2001; Niinemets, 2010). For instance, shade-tolerant trees have a higher branching density and a more voluminous crown (Mourelle et al., 2001). Finally, patch contrast, the

85   difference in composition and structure between forest and non-forested land, is another determinant

86   of the forest edge structure (Harper et al., 2005). Patch contrast, and in particular the contrast in

87   canopy height, is related to forest edge characteristics and composition but also to climate, since this

88   affects the productivity. In productive ecosystems (e.g. at lower latitude and elevations), patch

89   contrast in canopy height is expected to be higher (Esseen et al., 2016). Understanding how these

90   factors affect the structure and composition of forest edges is important, as ultimately the structure

91   will modify the edge functioning and habitat availability, making edges significantly different from

92   the forest interiors (Harper et al., 2005).

93   Both the three-dimensional structure as well as the tree species composition of forest edges can be

94   used as descriptors to better capture the biodiversity, nutrient cycling and microclimate in forest

95   edges. Complex edges with structurally diverse vertical layers provide shelter and different food

96   resources for a variety of species (Lindenmayer et al., 2000; Wermelinger et al., 2007). Hence, they

97   may thus act as local hotspots or potential refugia, on a longer term, for biodiversity (Goetz et al.,

98   2007; Zellweger et al., 2017; Melin et al., 2018). In terms of the understorey vegetation, Hamberg et

99   al. (2009) found that side-canopy openness, tree species composition and distance to the forest edge

100   were the main structural metrics affecting the understorey vegetation. Additionally, it has been

101   demonstrated that gradually building up the vertical complexity of forest edges (e.g. fringe, mantle

102   and shrub layer) mitigates the negative effects of atmospheric deposition (Wuyts et al., 2009). Finally,

103   forest edge structure and tree species composition also partly control the microclimatic differences

104   between the exterior and interior condition, and thus the establishment of a typical forest microclimate

105   (Young and Mitchell, 1994; Didham and Lawton, 1999; Davies-Colley et al., 2000; Schmidt et al.,

106   2019). From an open area onwards, gradients in temperature, light, humidity and wind are mediated

107   by the presence of a forest edge leading towards a moderate climate subject to less variability inside

108   the forest (Davies-Colley et al., 2000; Ewers and Banks-Leite, 2013). For example, organisms living

109   under a denser canopy layer experience lower maximum temperatures (Greiser et al., 2018; De Frenne

110   et al., 2019; Zellweger et al., 2019a) and higher minimum temperatures (Chen et al., 1999; Saunders

111 et al., 1999; De Frenne et al., 2019; Zellweger et al., 2019a) than organisms living near edges and in

112 fully open conditions. The main determinants of the forest microclimate are canopy openness and

113 cover (Ehbrecht et al., 2019; Zellweger et al., 2019a). In addition, structural metrics associated with

114 old growth forest (i.e. a tall canopy, vertical heterogeneous structure and high biomass) are known to

115 contribute to a higher buffering capacity (Frey et al., 2016; Kovács et al., 2017).

116 The forest edge provides many ecological processes that are directly associated and beneficial to

117 adjacent land uses and its structure influences the depth and magnitude of the edge influence on

118 ecosystem processes (Harper et al., 2005; Wuyts et al., 2009; Schmidt et al., 2019). Yet, large-scale

119 studies analysing the variation of the structure and tree composition of forest edges are lacking.

120 However, Esseen et al. (2016) studied the variability in forest edge structure across Sweden and

121 detected variation in multiple forest edge structural variables associated with edge origin, land use,

122 climate and tree species composition. Most of the other studies focusing on forest edge structure are

123 often system specific and performed at local scales, covering restricted spatial extents (Cadenasso et

124 al., 2003). To our knowledge, no continental-scale assessment of forest edge structure has been

125 undertaken so far. This is surprising, not only due to their importance, but also due to the high

126 plausibility that forest edges strongly vary in space and time (Schmidt et al., 2017).

127 Moreover, to date, when studying forest edges, most authors have only provided a relatively limited

128 description of the structure (Schmidt et al., 2019) which makes it hard to compare edge influences on

129 forest structure and composition (Harper et al., 2005). The development of new methods such as state-

130 of-the-art 3D terrestrial laser scanning (TLS, also referred to as terrestrial light detection and ranging

131 (LiDAR)) have made it possible to assess the vegetation structure in unprecedented nearly millimetre-

132 level accuracy (van Leeuwen and Nieuwenhuis, 2010; Liang et al., 2016). TLS is also beneficial due

133 to its rapid, objective and automatic documentation and more importantly the possibility to extract

134 non-conventional forest metrics (Dassot et al., 2011; Liang et al., 2016). Doing so, the vertical

135 distribution of plant material can be determined in high detail, which is an important characteristic of

136 the forest and edge structure and a significant driver of microclimate (Wang and Li, 2013; Frey et al.,

2016), habitat availability and biodiversity (Goetz et al., 2007; Melin et al., 2018). Therefore, TLS is increasingly used for inventorying a large number of sites in a comparable way, but very few studies have collected local TLS-data in a replicated design covering a large spatial extent (i.e. continental extent).

Here we quantified structural variation using conventional forest inventory techniques and state-of-the-art terrestrial laser scanning across 45 edge-to-interior transects in deciduous broadleaved forests along latitudinal and elevational gradients across Europe. Our major objective was to study the variation in forest edge structural metrics. We studied how large environmental gradients, driven by temperature and humidity, affected the edge structure (i.e. canopy cover, canopy openness, total basal area, stem density, mean diameter at breast height (DBH), the coefficient of variation of the DBH, plant area index, canopy height, the peak in plant material density and the height of this peak and finally the foliage height diversity). We expected to find structurally different forest edges across Europe, resulting from changes in the macroclimate (light, temperature and precipitation) similar to the global patterns in vegetation structure and composition (Aussenac, 2000; Quesada et al., 2012). A decrease in temperature and/or water availability could limit the productivity and thereby reduce, for instance, stem density, canopy height and the amount of plant material. Yet, even on a smaller spatial scale, the microclimate, could affect the vegetation structure and therefore we assumed to detect a changing forest structure from forest edge to interior. Additionally, we assessed what the effects of forest management were within the different regions via a replicated design covering contrasting management types per site. We assumed that management would shape the forest edge structure on a local scale. For example, intensive management (e.g. intensive thinnings) will reduce canopy cover, stem density and the amount of plant material but will increase the canopy openness. This could negatively affect the forest edge's capacity to reduce the impact of the surrounding land. Finally, we took the influence of tree species composition on the forest edge structure into account. We expected that more shade-tolerant species would form denser edges with a higher plant area index and vegetation cover and a lower canopy openness.

2. Material and methods

2.1 Study design and area

We studied forests along a latitudinal gradient from central Italy (42 °N) to central Norway (63 °N), crossing the sub-Mediterranean, temperate and boreonemoral forest biomes of Europe. This approximately 2300 km wide transect captures macroclimatic variation across Europe (Δ mean annual temperature ~ 13 °C). Along this south-north gradient, nine regions were selected (**Figure A1**): (1) Central Italy, (2) Northern Switzerland, (3) Northern France, (4) Belgium, (5) Southern Poland, (6) Northern Germany, (7) Southern Sweden, (8) Central Sweden and (9) Central Norway.

In three regions, i.e. Norway, Belgium and Italy, the study design was replicated along an elevational gradient covering low, intermediate and high elevational sites to include the climatic variation resulting from elevational differences (21 - 908 m above sea level, m a.s.l) with an expected Δ temperature ~ 5.76 °C (ICAO, 1993). For the six remaining regions, only lowland transects were studied (between 8 and 450 m a.s.l.).

In all 15 sites (i.e. nine lowland, three intermediate and three high-elevation sites), we collected data in three forest stands with a distinct management type. The first type was always a dense and vertically complex forest with a well-developed shrub layer, since it had not been managed for more than 10 years and in general not thinned for at least three decades. A high basal area and canopy cover characterized this type of forest stands, hereafter always referred to as 'dense forests'. A second type, 'intermediate forests', comprised stands with a lower basal area and canopy cover, resulting from regularly thinning (last time approximately five to 10 years ago). The shrub layer in these stands was sparse or absent. The third management type represented 'open forests' with a low basal area and higher canopy openness. These forests were intensively thinned in the recent past (one to four years before sampling). Therefore, these forests were structurally simple with no shrub and subdominant tree layer. The studied forests thus represent a 'chronosequence' of forest management types along the typical gradient of a management cycle of managed ancient deciduous forests in Europe.

188   We focused on mesic deciduous forests on loamy soils, in general dominated by oaks (mainly

189   *Quercus robur, Quercus petraea* or *Quercus cerris)* because these are hotspots for biodiversity,

190   constituting an ecologically important forest type and represent a substantial portion of the deciduous

191   forests across Europe (Bohn and Neuhäusl, 2000; Brus et al., 2012). Other important tree species

192   were *Fagus sylvatica*, *Betula pubescens*, *Populus tremula*, *Ulmus glabra*, *Alnus incana* and *Carpinus*

193   *betulus*. One up to ten different tree species were present per forest stand. All forests were larger than

194   4 ha, and ancient (that is, continuously forested and not converted to another land use since the oldest

195   available land use maps which is typically at least 150-300 years). We selected the three forest stands

196   that best matched the list of selection criteria after multiple field visits (**Appendix A1**), often with

197   assistance from local forest managers, who had knowledge of the area and the historical land-use.

198   *2.2 Edge-to-interior transects*

199   In each forest, we studied a 100 m-long edge-to-interior gradient. In total, 45 edge-to-interior transects

200   (15 sites and 3 replicates covering the management types per site, **Table A1**) were established, all

201   starting at a southern forest edge to standardize the edge orientation. The studied edges were bordered

202   by arable land or grassland, as is common in highly fragmented landscapes in Europe, and all plots

203   were at least 100 m away from any other forest edge. Each transect encompassed five 3×3 m² plots

204   (thus resulting in 225 plots), all at a fixed distance perpendicular to the edge according to an

205   exponential pattern. The centre of the first plot was located at a distance of 1.5 m from the outermost

206   line of tree trunks, followed by plots centred at 4.5 m, 12.5 m, 36.5 m and 99.5 m from the forest edge

207   towards the interior. If a forest trail was present, we slightly moved the plot away from the trail to

208   avoid effects on the vegetation structure (this was the case in only six plots and never in the two plots

209   closest to the edge).

210   *2.3 Forest structure characterisation*

211   The forest structure was quantified between May and July 2018 (leaf-on conditions). Characterisation

212   of the forest structure in each plot was done both via a conventional forest inventory survey and via

213   state-of-the-art TLS.

2.3.1 Conventional forest inventory survey

The species-specific percentage cover of all shrub (1 – 7 m) and tree (> 7 m) species was visually estimated (resolution 1 %) within each 3×3 m² quadrat. The total vegetation cover was calculated as the cumulative sum of each of the individual tree and shrub species co-occurring within a given quadrat, thus allowing the total cover to exceed 100 % due to overlap as is common in forests (Zellweger et al., 2019a). Next, the centre of each quadrat served as the centre of a larger circular plot with a radius of 9 m. An ultrasound hypsometer (Vertex IV, Haglöf, Sweden) was used to determine the plot dimensions. In these plots, we measured the diameter at breast height (DBH, 1.3 m) of all trees (with DBH $\geq$ 7.5 cm) with a caliper via two DBH measurements per stem perpendicular to each other. We then calculated the mean DBH per plot and its coefficient of variation (CV). Further, total basal area and stem density per hectare were calculated at plot level. As part of the first and second circular plots extended beyond the forest edge and measurements stopped at the edge (due to the obvious absence of trees), the total basal area and stem density were recalculated for the fraction of forested area. Finally, canopy openness was determined with a convex spherical densiometer (Baudry et al., 2014). Canopy openness at plot level was calculated as the average of three readings: one in the plot's centre and two at a distance of 4.5 m left and right of the centre (following a line parallel to the forest edge), respectively. In sum, we derived six response variables via the conventional field inventory: total vegetation cover, mean DBH, the CV of the DBH, total basal area, stem density and canopy openness.

2.3.2 Terrestrial laser scanning

At each plot, we carried out a single-scan position TLS using a RIEGL VZ400 (RIEGL Laser Measurement Systems GmbH, Horn, Austria) to map the complex three-dimensional structure of the forest plot. The instrument has a beam divergence of nominally 0.35 mrad and operates in the infrared (wavelength 1550 nm) with a range up to 350 m. The pulse repetition rate at each scan location was 300 kHz, the minimum range was 0.5 m and the angular sampling

resolution was 0.04°. Scanning from one single independent location, instead of processing

multiple scanning positions, ensures an objective and holistic observation of forest stand

structure while being less time consuming compared to multiple scanning positions (Calders

et al., 2014; Seidel et al., 2016). The scanner was mounted on a tripod (1.3 m above the

ground) and placed in the centre of each plot, where one upright and one tilted scan (90° from

the vertical) were taken. These two scans were co-registered, and their data was merged to

one point-cloud making use of matrices calculated in the RISCAN Pro software and six

reflective targets placed around each of the plots before scanning. The reflectors were used to

link and merge the upright and tilted scan as they represent exactly the same locations in both

images. Based on the resulting raw point cloud data, a local plane fit was executed to correct

for topographic effects. Two adjustments were made to the method described by Calders et

al. (2014). Firstly, for the topography correction with TLS plane fitting, a reduced grid (10 m

by 10 m) around the scan position was applied. Herein, the lowest points (i.e. ground points)

were selected with a 1 m spatial resolution. Secondly, the iterative reweighted least squares

regression, accustomed to weight and thus correct for scanner distance of the ground points,

was omitted. After performing a local plane fit, vertical profiles of plant area per volume

density ($m^2\,m^{-3}$) (PAVD) as a function of the height were constructed for each plot from the

adjusted point cloud. These profiles were based on the gap fraction or the gap probability that

represents the probability of a very narrow beam to miss all scattering elements in the forest

and escape through the canopy without being intercepted by foliage or wood. Calculation of

the gap probability and subsequently the vertical plant profiles is explained in Calders et al.

(2014) and was executed in Python making use of the Pylidar library

(http://www.pylidar.org/en/latest/). Subsequent calculations to derive the respective variables

were done in R (R Core Team, 2019). PAVD-profiles illustrate the plant canopy structure and

are often used to study the vertical organisation of plant material from the forest floor to the

top of the canopy (Calders et al., 2014). Based on the profiles, we extracted several forest

266   structural metrics. Firstly, we determined the plant area index (PAI), which is the total area of

267   woody (e.g. branches and stems) and non-woody biomass (i.e. leaves) per unit of surface area.

268   The PAI was determined at plot level as the integral of the PAVD over the canopy height.

269   Secondly, a canopy related structural metric, namely canopy top height was extracted. Canopy

270   top height was based on the 99 % PAVD-percentile to remove atmospheric noise.

271   Consequently, the peak in PAVD or thus the maximum density and its height were derived

272   from the profiles. We also quantified the vertical heterogeneity in plant material along the

273   profile, namely, the foliage height diversity (FHD). The FHD was calculated as the Shannon-

274   Wiener index for diversity, *sensu* MacArthur and MacArthur (1961):

275
$$FHD = -\sum_i p_i \times \log p_i$$

276   With p_i representing the proportion of plant material in the ith 1 m vertical layer (i.e. PAVD

277   for a given 1 m vertical layer).

278   A vertically simple profile will receive a low FHD-value while the value will increase with

279   increasing heterogeneity of the FHD. Lastly, canopy openness was calculated as the average

280   percentage of gap fraction across the angle 5-70°. In total, six TLS-based response variables

281   were extracted: PAI, canopy top height, the peak in PAVD, the height of this peak, FHD and

282   canopy openness.

283 *2.4 Macroclimatic predictor variables*

284 Meteorological data were downloaded from CHELSA (version 1.2, average climatic conditions over

285 the period 1979-2013 at a spatial resolution of 30 arc sec, equivalent to approximately a 0.5 km^2

286 resolution at 50 °N) (Karger et al., 2017). We extracted the mean annual temperature (MAT, °C) and

287 the mean total annual precipitation (MAP, mm/year) for each site. Subsequently, we calculated the

288 de Martonne Aridity Index (DMI), a drought index based on the MAP divided by the MAT plus 10

289 °C (de Martonne, 1926). High values express a high humidity while areas with water stress are

290 characterized by low values.

291 *2.5 Data analysis*

292 Variation in forest edge structural metrics across Europe was analysed in R (R Core Team, 2019)

293 making use of linear mixed-effect models (Zuur et al., 2009) and the *lmer* function in the R-package

294 *lme4* (Bates et al., 2015). In all models, region and transect nested within region were added as

295 random effect terms (i.e. random intercepts, as 1│region/transect in R syntax) to account for spatial

296 autocorrelation due to the hierarchical structure of the data; three up to nine unique transects were

297 nested within each region and thus tend to be more similar than transects from another region.

298 In a first set of models, the fixed effects were our four design variables (i.e. latitude, elevation,

299 management type and distance to the edge), including all two-way interactions. Finally, also the

300 community-weighted mean shade tolerance of each plot was added to each model as a covariate.

301 At the local scale, both tree species richness and composition differed across the transects and sites

302 and this could affect the forest structure since tree species differ in their architectural characteristics

303 (Mourelle et al., 2001; Niinemets, 2010). To better account for differences in tree species community

304 composition and their effect on the forest structure and to avoid the detection of patterns in edge

305 structure that are only related to tree species identity or forest development stage, the tree community-

306 weighted mean shade tolerance was used as a predictor. The shade tolerance index (Niinemets and

307 Valladares, 2006) ranges between one and five and describes the tolerance of tree and shrub species

308 to grow in the shade. Very shade-intolerant species (e.g. *Betula pubescens)*, requiring high levels of

309 light (> 50 %) to grow, receive a low value (minimum 1) while the opposite (maximum 5 for a 2-5 %

310 light availability) is true for very shade-tolerant species (e.g. *Fagus sylvatica*) (Niinemets and

311 Valladares, 2006). Even though shade tolerance is mainly determined on juveniles, the relative

312 ranking amongst co-existing species stays overall very similar for adults (Grubb, 1998; Niinemets

313 and Valladares, 2006). The shade tolerance was calculated at the plot level and was based on all tree

314 species in the plot weighted by their respective cover in the conventional inventory. The equation

315 below summarises our first set of mixed-effect models, whereby x represents the twelve forest

316 structural metrics.

$$x \sim (latitude \times elevation) + (latitude \times management\ type) + (latitude \times distance\ to\ the\ edge)$$
$$+ (elevation \times management\ type) + (elevation \times distance\ to\ the\ edge)$$
$$+ (management\ type \times distance\ to\ the\ edge) + shade\ tolerance + (1|region/transect)$$

To achieve a more profound understanding of the patterns and their drivers, two additional sets of models were constructed where latitude and elevation were substituted first by the MAT and secondly by the DMI. Each time management type, distance to the edge and the community-weighted mean shade tolerance of the tree layer were retained as fixed effects and region and transect nested within region as random effects. Two-way interactions were allowed between substitutes and design-variables as well as amongst design variables.

Since the distribution of our plots follows an exponential pattern, the distance to the edge was log-transformed prior to the analyses. All continuous predictor variables were standardized (z-transformation) to allow for a better-standardized comparison of model coefficients. Two response variables, canopy openness derived via TLS and canopy openness derived via the densiometer, had right-skewed distributions and were log transformed prior to the analyses. For each of the above-mentioned combinations of response variables and models, a backward model selection was executed whereby non-significant effects and/or interaction terms were removed using the *step*-function of the R-package *lmerTest* (Kuznetsova et al., 2017). After model selection, restricted maximum likelihood was employed to assess the model parameters and finally, we corrected our *p*-values for multiple comparison testing making use of false discovery rates (FDR). The FDR is the estimated proportion of Type 1 errors or thus the proportion of comparisons that are wrongly called significant (Pike, 2011). Throughout the text, we will always refer to the corrected *p*-values but asterisks in all tables indicate original *p*-values. The proportion of the explained variance by the fixed effects only (i.e. marginal R^2) and the combination of fixed and random effects (i.e. conditional R^2) determined the model fit. To better understand how strong variables at the edge differed from those at the interior, the magnitude of edge influence (MEI) was calculated as well. The MEI was estimated as (edge –

344   interior)/ (edge + interior) for all response variables but separately per management type. The

345   resulting value fluctuates between -1 and 1 whereby 0 represents no edge influence (Harper et al.,

346   2005). Finally, potential associations between predictor variables as well as amongst response

347   variables were identified with Pearson correlations.

3 Results

An overview of the twelve response variables and their mean and standard deviation in each region can be found in **Table 1**. For almost all variables, there was a high variability between and within regions, as indicated by the differences in mean values and standard deviations, respectively. For instance, there were large differences in stem density; in Norway, the average stem density was the highest whereas France had the lowest stem density. The average basal area on the other hand, was highest in Switzerland and Southern Sweden. In Germany, average canopy cover was the highest and canopy openness the lowest whereas the opposite, the lowest canopy cover and highest canopy openness was found in France. Average canopy openness determined with TLS was also the highest in France but lowest in Switzerland and Germany. Variation between regions and between management types were visualised in the PAVD-profiles (vertical plant profiles form which most of our TLS-variables were derived) in **Figure B1** and **Figure 1** as well. Further, between- and within-site variability in the dominant tree and shrub species was found (**Table A1**). Oaks dominated most of the transects but the species differed between regions (e.g. *Quercus cerris* in Italy whereas in Belgium *Quercus petraea* and *Quercus robur* were the most dominant). In Norway, the dominant tree species were *Alnus incana*, *Ulmus glabra* and *Betula pubescens*.

Our first set of models, including the four design variables latitude, elevation, management type and distance to the edge in addition to the mean community-weighted shade tolerance of the tree layer (**Table 2**) showed that the forest structure varied strongly with the distance to the edge. Interestingly, in a few cases, these edge-to-interior gradients depended on one of the other design variables; we found significant interactive effects of the distance to the forest edge with latitude, elevation and/or management. For instance, for the PAI and stem density, we found an interaction effect of distance to the forest edge with management and latitude, respectively. Dense forests exhibited an extended and gradual increase in PAI from the edge to the interior, whereas this increase was weaker in open forests ($p = 0.090$) and significantly more abrupt and shorter in intermediate forests ($p = 0.022$, **Table**

373 **2 and Figure 2**). This results in a flatter and quicker saturated edge-to-interior gradient for

374 intermediate forests.
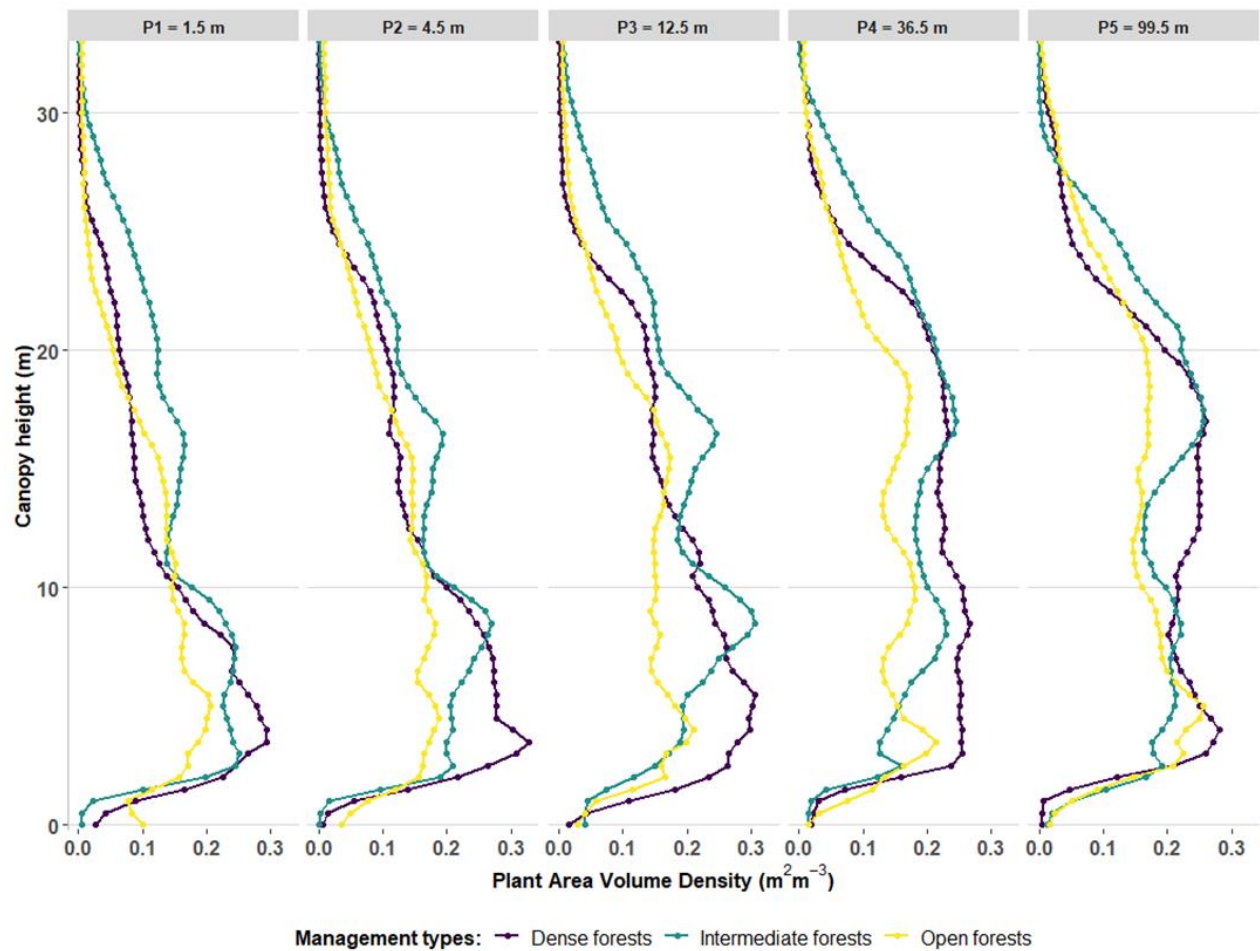
375

376 *Figure 1:* Vertical profiles of plant area per volume density (PAVD) (m^2 m^{-3}) at different distances from the edge

377 (1.5–99.5 m) for three management types. The profiles were averaged across all regions and elevations (n = 15) with

378 management type shown in different colours. **Figure B1**, in the appendix, shows the PAVD-profiles for the nine regions,

379 averaged across all management types and elevations.

Table 1: Overview of the response variables per region (mean ± standard deviation). PAVD = plant area volume density.

Region	Variables from the conventional forest inventory						Variables from TLS					
	Total cover (%)	Canopy openness (%)	Total basal area (m² ha⁻¹)	Stem density (ha⁻¹)	Mean DBH (cm)	Coefficient of variation DBH	Plant area index	Canopy height (m)	Maximum PAVD (m²m⁻³)	Height peak PAVD (m)	Canopy openness (%)	Foliage height diversity
Central Italy	106.6 ± 37.5	12.5 ± 6.9	24.3 ± 11.7	923 ± 661	18.8 ± 6.6	46 ± 16	3.79 ± 0.81	19.7 ± 5.1	0.25 ± 0.11	10.1 ± 6.2	7.96 ± 4.76	2.72 ± 0.33
Northern Switzerland	136.0 ± 44.4	5.0 ± 2.1	47.0 ± 24.2	582 ± 268	29.2 ± 11.11	63 ± 21	5.09 ± 1.21	29.6 ± 3.8	0.23 ± 0.11	8.7 ± 8.6	2.49 ± 1.77	3.25 ± 0.23
Northern France	89.0 ± 72.9	29.4 ± 32.4	28.7 ± 12.4	280 ± 269	41.6 ± 17.8	66 ±26	3.43 ± 2.43	33.6 ± 3.8	0.12 ± 0.09	14.3 ± 11.8	24.34 ± 27.26	3.35 ± 0.13
Southern Poland	108.7 ± 36.1	12.0 ± 5.7	25.2 ± 11.4	575 ± 246	22.1 ± 6.5	41 ± 12	4.22 ± 1.11	24.9 ±2.2	0.21 ± 0.06	13.5 ± 8.0	5.95 ± 5.57	3.00 ± 0.11
Belgium	121.1 ± 38.1	5.3 ± 4.6	34.0 ± 23.1	579 ± 449	27.9 ± 15.2	59 ± 24	4.57 ± 1.62	24.5 ± 3.6	0.23 ± 0.10	10.4 ± 7.0	6.03 ± 9.08	2.99 ± 0.22
Northern Germany	153.9 ± 41.4	1.7 ± 2.1	37.9 ± 15.7	402 ± 224	33.8 ± 12.3	56 ± 16	5.22 ± 1.31	25.1 ± 1.6	0.27 ± 0.08	13.9 ± 9.9	2.91 ± 4.36	3.01 ± 0.12
Southern Sweden	128.0 ± 68.9	6.2 ± 5.0	46.3 ± 31.0	386 ± 209	34.7 ± 10.3	60 ± 34	5.30 ± 0.96	25.3 ± 3.1	0.28 ± 0.10	12.3 ± 9.8	4.08 ± 5.71	3.00 ± 0.11
Central Sweden	113.5 ± 40.3	3.7 ± 3.2	38.1 ± 31.1	348 ± 200	41.9 ± 37.5	50 ± 28	3.61 ± 1.29	25.4 ± 1.7	0.17 ± 0.07	9.4 ± 7.1	7.95 ± 5.34	3.03 ± 0.07
Central Norway	115.0 ± 39.7	7.8 ± 8.5	32.8 ± 15.6	1528 ± 849	15.4 ± 3.3	47 ± 17	3.68 ± 1.37	15.2 ± 4.3	0.26 ± 0.09	7.4 ± 4.8	11.50 ± 16.88	2.48 ± 0.32

Table 2: Summary of the results (after model selection) of the first set of models where we tested the impact of the four design variables (e.g. latitude, elevation, management and distance to the forest edge). Variables derived via conventional forest inventory techniques are depicted above the double line, while the TLS-based variables are shown below the double line. Both estimates and p-values including false discovery rate correction (FDR) of the parameters are shown, original p-values before FDR-correction are shown as asterisks between brackets ($p < 0.05$*, $p < 0.01$**, $p < 0.001$***). Dense forests were used as the reference management type. The proportion of variance explained by the random factors, the marginal R^2, and the proportion of the variance explained by both random and fixed effects, the conditional R^2, are also shown.

Response variable		Latitude	Elevation	Distance to the edge	Inter-mediate	Open	Shade tolerance	Lat. × Distance	Elev. × Distance	Inter-mediate × Distance	Open × Distance	Elev. × Inter-mediate	Elev. × Open	Marginal R^2	Conditional R^2
Total cover	Estimate				-14.05	-31.65								0.08	0.41
	p-value				0.908	0.051 (**)									

Canopy openness	**Estimate**				0.15	0.68	-0.45								0.14	0.59
	p-value				0.992	< 0.001 (***)	< 0.001 (***)									
Total basal area	**Estimate**	3.44	-1.19	-7.76	2.36	-8.30	4.63		2.31						0.27	0.38
	p-value	0.078 (*)	0.777	< 0.001 (***)	0.777	0.078 (*)	0.005 (**)		0.078							
Stem density	**Estimate**	193.91	87.89	-162.40	-22.79	-361.37		-115.25	-68.19						0.21	0.75
	p-value	0.443	0.443	< 0.001 (***)	1.000	0.055 (*)		< 0.001 (***)	0.015 (**)							
Mean DBH	**Estimate**		-1.80	-0.94					1.95						0.03	0.50
	p-value		0.960	0.907					0.081 (*)							
Coefficient of variation DBH	**Estimate**	-0.77		0.45				2.83							0.02	0.33
	p-value	1.000		1.000				0.131 (*)								
Plant area index	**Estimate**		-0.22	0.65	0.15	-0.92	0.25		-0.12	-0.37	-0.27				0.30	0.66
	p-value		0.190	< 0.001 (***)	0.888	0.029 (*)	0.022 (**)		0.089 (*)	0.022 (**)	0.090					
Canopy height	**Estimate**		0.28	0.64	0.14	0.46	0.48					-3.04	-0.84		0.10	0.91
	p-value		1.000	< 0.001 (***)	1.000	1.000	0.103 (*)					0.089 (*)	1.000			
Maximum PAVD	**Estimate**		0.01	0.02					-0.01						0.05	0.45
	p-value		1.000	0.001 (***)					0.187 (*)							
Height peak PAVD	**Estimate**	-1.33	-1.40	2.30	3.86	1.15									0.17	0.34
	p-value	0.142	0.139 (*)	< 0.001 (***)	0.079 (*)	0.945										
Canopy openness	**Estimate**		0.23	-0.16	0.01	0.87	-0.33		0.11						0.29	0.62
	p-value		0.110	0.007 (**)	1.000	0.010 (**)	< 0.001 (***)		0.079 (*)							
Foliage height diversity	**Estimate**		-0.08	0.02											0.06	0.84
	p-value		0.220	0.156 (*)												

387

388
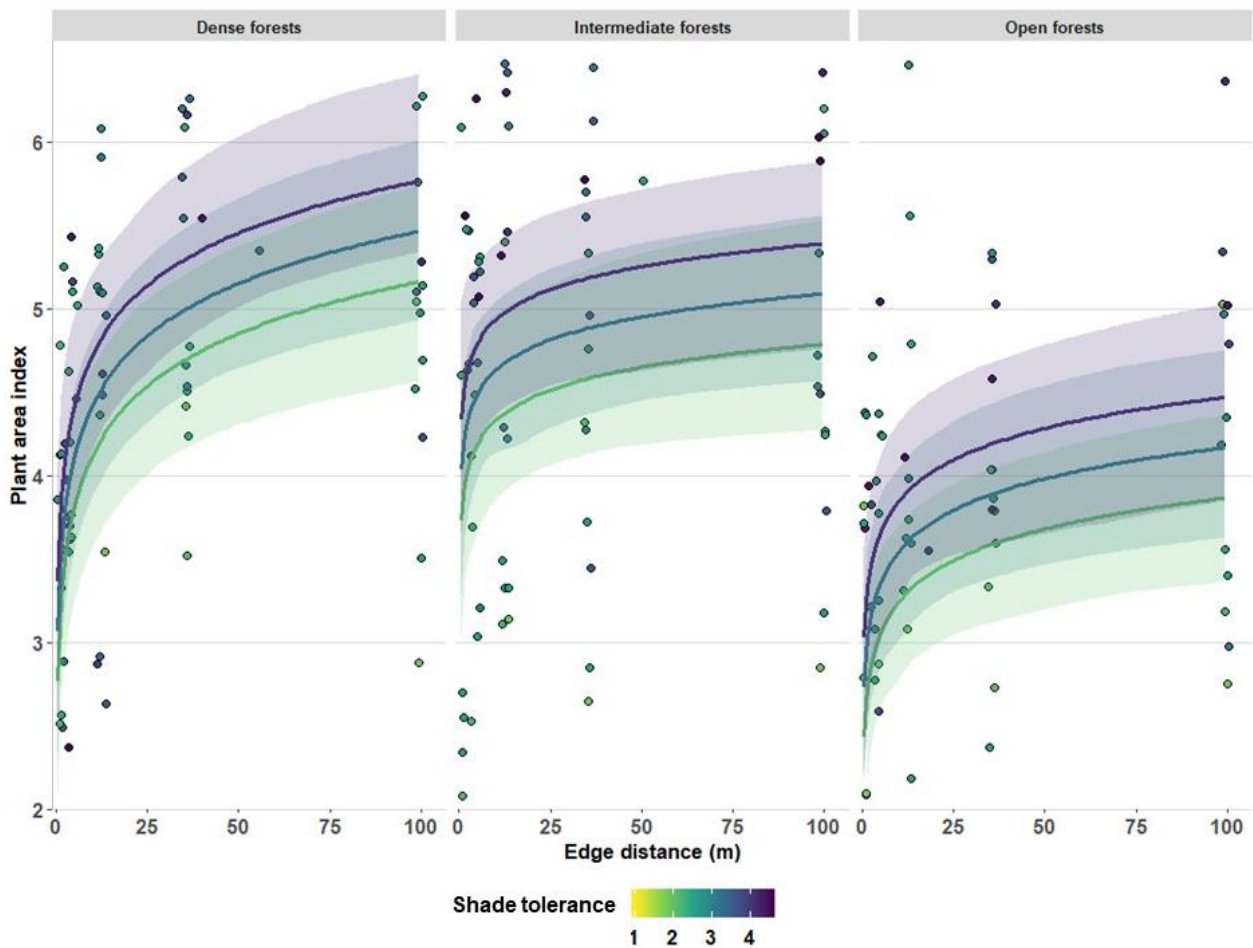
Figure 2: Plant area index (PAI; mean and 95 % predictions intervals) as a function of the distance to the forest edge (m)
for three management types. The lines show the model predictions of the interaction between distance to the edge and
management. Different colours represent the shade tolerance of the tree layer (values close to one denote low shade
tolerance; values close to five a high shade tolerance). Dots indicate the raw data points; a small amount of noise was
added along the X-axis to improve clarity.

Moreover, we detected a decrease in stem density from edge to interior, but this decrease was stronger
at northern latitudes and flattened out towards southern Europe ($p < 0.001$, **Figure 3, Table 2**).
Furthermore, a higher community-weighted mean shade tolerance was found under closed canopies
(densiometer and TLS, $p < 0.001$ for both) and basal area ($p = 0.005$) and the PAI ($p = 0.022$, **Figure
2**) were higher when shade tolerance increased (**Table 2**). For canopy openness, we found no edge-
to-interior gradients when assessed by means of the densiometer, whereas these gradients were
significant when quantified with TLS ($p = 0.007$, **Table2**).

401
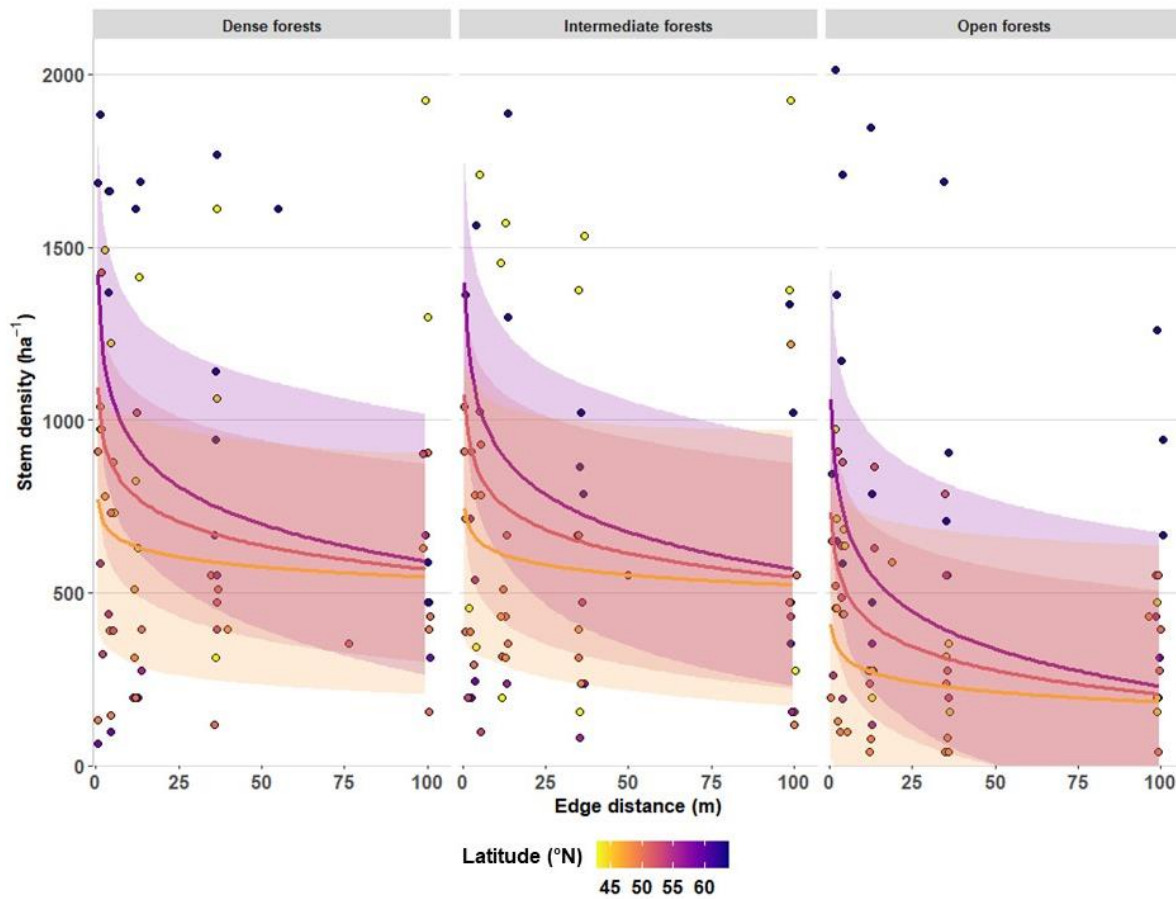
Figure 3: Stem density (mean and 95 % prediction intervals) as a function of distance to the edge (m) for three management types. The lines represent the model predictions of the interaction between distance to the edge and latitude; the colours illustrate the influence of a varying latitude. Elevation was set at its median value when plotting the lines. The dots show the raw data points; a small amount of noise was added along the X-axis to improve clarity.

For our second set of models, where the MAT replaced elevation and latitude to assess macroclimate temperature effects, we found a significant interaction between MAT and the distance to the forest edge ($p < 0.001$, **Table B1**) for stem density. As in the first model, there was a strong decrease in stem density from edge to interior in cold regions whereas the decrease was less distinct in warm regions (**Figure B2, Table B1**). The results for the PAI were analogous to the first model as well. Edge-to-interior gradients in PAI were significantly weaker in intermediate forests ($p = 0.019$) in comparison with dense forests (**Table B1**). Additional significant distance to edge effects were found for the TLS derived canopy openness ($p = 0.01$) (not for canopy openness determined with the densiometer), basal area ($p < 0.001$), canopy height ($p < 0.001$), the peak in PAVD ($p = 0.001$) and the height of the peak in plant material ($p < 0.001$).

In a final set of models, we replaced the MAT by the DMI (de Martonne Aridity Index, **Table B2**) to assess macroclimate drought effects. After model selection, DMI was retained as a predictor of the stem density, canopy height and FHD. For the stem density, DMI showed one significant interaction, namely with distance to the edge ($p < 0.001$, **Table B2**); in areas with a higher humidity, stem density decreased more sharply from edge to interior than in regions with a lower DMI (**Figure B2, Table B2**). For both canopy height and FHD there were marginally significant interaction effects between DMI and the distance to the forest edge. The increase in canopy height ($p = 0.070$, **Figure 4**, **Table B2**) and FHD ($p = 0.057$, **Figure B3, Table B2**) from forest edge to interior was more pronounced in very humid areas.

Besides a marginally significant interaction with distance to the forest edge, an interaction effect between DMI and forest management was found for both canopy height and FHD. Open forests had a higher canopy height and higher foliage height diversity (that is, higher complexity) in drier areas in comparison to intermediate or dense forests. In regions where there was a very high water availability, the opposite was found, namely a higher canopy height and FHD for the dense and intermediate forests ($p = 0.044$ for canopy height, **Figure 4, Table B2** and $p = 0.067$ for FHD, **Figure B3, Table B2**). Finally, the PAI and canopy openness were not affected by the DMI. However, for the PAI we found a more or less similar interaction effect of management and distance to the forest edge as in the previous two models (**Table 2, B1 and B2**).

Similar results were found for the magnitude of edge influence (MEI). The MEI varied across management types and depended on the studied variable (**Figure B4**). Total basal area and stem density show a high positive MEI, whereas for the PAI the MEI is negative. The average MEI for the PAI was shorter in intermediate than in open or dense forests. For some variables (e.g. total cover, canopy openness determined with the densiometer, mean DBH and FHD), the MEI was close to zero.

439
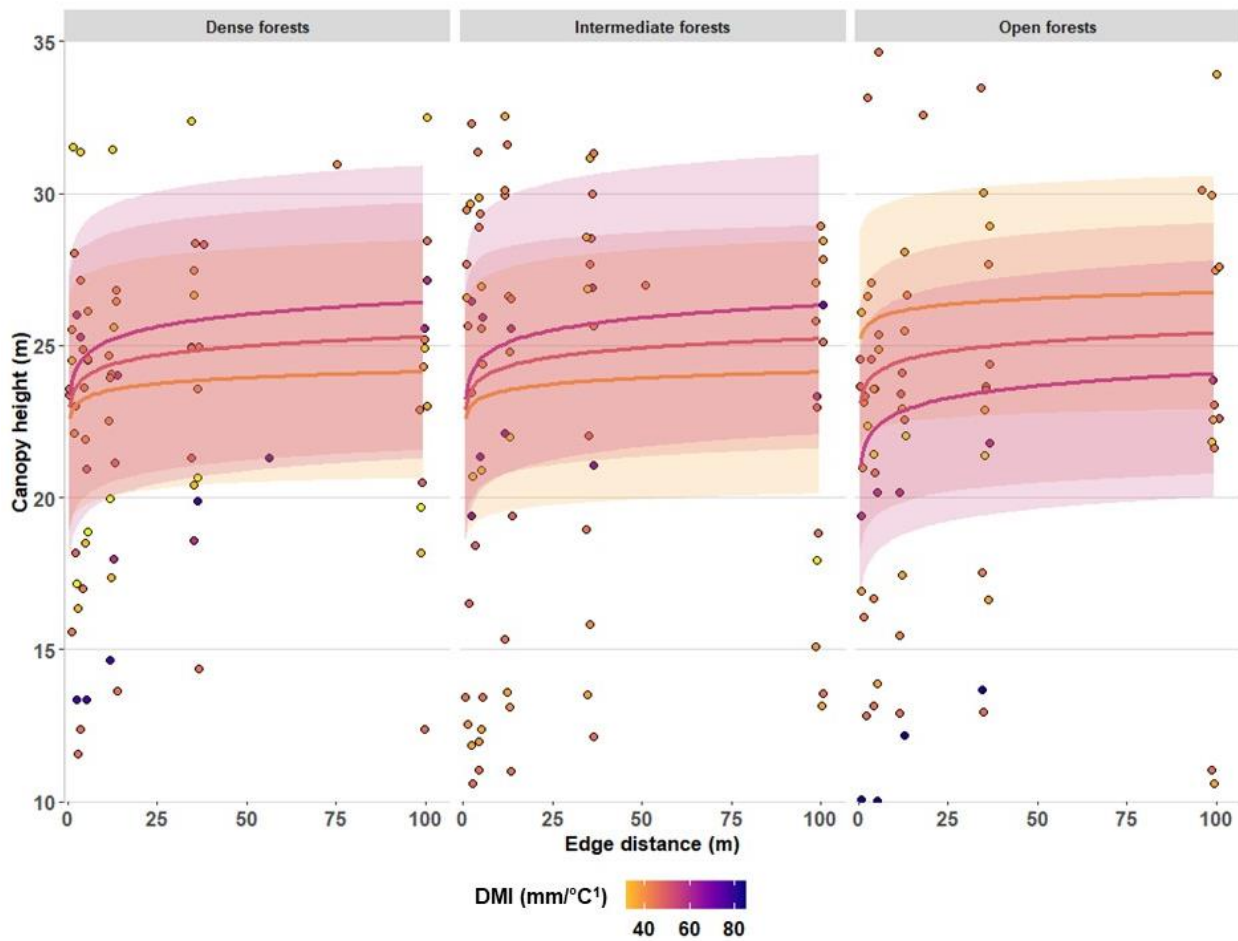
Figure 4: Canopy height (mean and 95 % prediction intervals) in function of the distance to the edge (m) for three management types. The lines show the model predictions of the interaction between water availability (DMI) and management, as well as between water availability and distance to the edge. Colours illustrate the impact of the DMI. Shade tolerance was set at its median value when plotting the lines. The dots show the raw data points; a small amount of noise was added along the X-axis to improve clarity.

4   Discussion

We found that the macroclimate, distance to the edge, forest management and tree species composition all influenced the forest edge structure across Europe. However, we also detected interactive effects of our predictor variables; latitude, mean annual temperature, humidity and management affected edge-to-interior gradients in the forest structure. In addition, we showed that management and humidity simultaneously influenced the forest edge structure.

4.1 The plant area index

The PAI increased towards the forest interior, independent of latitude, MAT or DMI, but was affected by management. The PAI was the lowest in the interiors of open forests (recently thinned forests) and increased towards dense forests. Forest management practices, directly via the removal of stems or indirectly via, for instance tree damage and mortality after management practices (Esseen, 1994; Laurance et al., 1998; Harper et al., 2005; Broadbent et al., 2008), can of course reduce the amount of plant material, followed by a subsequent recovery through increased productivity and regeneration in forest gaps. More interestingly, the interactive effects between management and distance to the forest edge were also significant. The build-up of the biomass towards the interior was more abrupt and quicker saturated in intermediate forests whereas more gradual edges were found both in dense and in open forests. Additionally, the average MEI was also shorter in intermediate forests. A possible explanation for this flatter edge-to-interior gradient in intermediately dense forests can be that there is an enhanced productivity of the remaining trees especially near the forest edge due to a higher resource availability (Smith et al., 2018), weakening the gradual increase in PAI as observed in dense forests or as seen in the first years after harvest (open forests).

Tree species composition could further influence these patterns. Our results support a positive effect of shade tolerance on the PAI. Shade-tolerant species (e.g. *Fagus sylvatica*, shade tolerance index of 4.56 ± 0.11) can cope with more shade (Niinemets and Valladares, 2006) and have a different crown geometry with a more voluminous crown (Canham et al., 1994; Mourelle et al., 2001) and a higher

470   branching density (Mourelle et al., 2001), creating a more filled and denser canopy. Progressively

471   increasing shade tolerance from edge to interior could therefore create an even smoother and gradual

472   forest edge.

473   *4.2 Stem density and basal area*

474   Higher stem densities at the edge might be due to better regeneration in response to the increased

475   light availability (Palik and Murphy, 1990). Especially noteworthy is that the decreasing trend is

476   stronger in northern than in southern Europe. This may result from the lower solar angles at northern

477   latitudes, which particularly increases light availability at the southern forest edge (Hutchison and

478   Matt, 1977; Harper et al., 2005). In the south, however, the received solar energy per surface unit is

479   higher and differences between edge and interior are less distinct. Here we noticed almost no

480   difference in stem density between edge and interior. Stronger decreases in stem density were also

481   detected in colder regions and regions with a higher water availability due to a strong negative

482   correlation between latitude and MAT and a strong positive correlation between latitude and DMI

483   (**Figure B5**).

484   In response to a lower tree density, we can expect an increased light availability resulting in higher

485   diameter increments (Harrington and Reukema, 1983; Ginn et al., 1991; Aussenac, 2000). Based on

486   the mean DBH or its CV, however, we did not find an impact of management. As a result of the

487   combined impact of a decreasing stem density and a more or less constant DBH, basal area decreased

488   towards the forest interior as previously described by Young and Mitchell (1994).

489   *4.3 Canopy openness*

490   Remarkably, results of canopy openness assessed via TLS and via the densiometer were slightly

491   different. The main difference was that TLS-based canopy openness depended on the distance to the

492   forest edge, whereas no edge impact was found for the densiometer-based openness. Densiometer

493   measurements are visual estimates and are therefore prone to biases related to observer errors,

494   differences amongst operators and a poor resolution (Jennings et al., 1999; Baudry et al., 2014). In

addition, the difference between the two approaches might be caused by scale issues as the scale of the two measurements differed. The densiometer measurements had an intermediate angle of view (< 60°) (Baudry et al., 2014) while TLS-derived canopy openness took into account a larger field of view (5 – 70°), possibly giving a more detailed representation of the openness and leading to the detection of edge-to-interior-patterns (i.e. a decrease in canopy openness with increasing distance to the forest edge). TLS derived canopy openness might thus be a better tool to study the canopy openness in a more detailed and objective way. Likewise, Seidel et al., (2011) state that especially TLS is recommended when high-resolution canopy information is required.

4.4 Canopy height and the FHD

Canopy height was slightly lower at the forest edge. This could be attributed to an increased wind speed near forest edges, resulting in canopy damage and a reduced canopy height (Laurance et al., 1998; Magnago et al., 2015). Nevertheless, we found that this edge-to-interior gradient in canopy height was affected by gradients in water availability; under conditions of low water availability forests had a lower canopy height likely due to competition for resources. Previous research showed that thinning can reduce canopy height due to a lower competition and the redistribution of nutrients to lateral branches or the trunk (Harrington and Reukema, 1983; Aussenac, 2000). We found such a lower canopy height with management, except in forests with a lower water availability. In drier regions, open, recently managed, forests had a higher canopy height than dense forests. In areas with a higher humidity, the opposite pattern was observed. One possible reason might be that a heavy thinning in a drier area could cause a strong reduction in competition, a drop in total water use and an increased throughfall. Hence, an increase in water availability might benefit the canopy height of the residual trees (Stogsdili et al., 1992; Aussenac, 2000).

Alternatively, canopy heights might be underestimated in dense forests due to shading by a higher number of stems and branches in the lower canopy layers (Watt and Donoghue, 2005; Liang et al., 2016; Muir et al., 2018). This means that the detection of the top of the canopy could be more accurate in drier and open forests, potentially leading to a higher estimated canopy height. Occlusion, the

521 inability to detect remote plant material due to dense vegetation close to the scanner, is especially an

522 issue when using a single scan position and can be reduced by using multiple scanning positions,

523 which is more time consuming and therefore not done in our study (van Leeuwen and Nieuwenhuis,

524 2010; Liang et al., 2016; Wilkes et al., 2017).

525 When tree height increases, the amount of plant material rises and so does the vertical heterogeneity

526 (Müller et al., 2018). We indeed found a strong positive correlation between canopy height and FHD

527 (**Figure B5**) and similar predictors for the FHD and canopy height were retained in our third model.

528 We found that the FHD in open forests was lower than in dense forests in regions with a high water-

529 availability, whereas the opposite was found for areas with a lower humidity. This could be due to a

530 higher canopy in drier and open forests, and thus a higher number of vertical layers in the calculation

531 of the FHD. A potential solution could be to select an equal number of height classes for all canopies

532 instead of working with 1 m bins. However, in our case, this was considered too complicated due to

533 the large range of canopy heights present in the dataset (9.5 up to 39 m) and because, up to now, there

534 is no generally accepted method for the delineation of height classes in the FHD-calculation

535 (McElhinny et al., 2005). Another downside of using the FHD as a metric of complexity is its

536 dependency on the relative amount of plant material in each layer. A high FHD does not always mean

537 a high complexity per se, but could result from a uniform filling of the vertical layers and not of a

538 heterogeneous canopy (Seidel et al., 2016).

539 *4.5 Management and ecological implications*

540 Our results demonstrate that the geographical position and macroclimate affect the forest edge

541 structure. Southern forests and forests in regions with a high MAT could be more susceptible to

542 influences from the non-forest environment (e.g. an increased atmospheric deposition and influx of

543 fertilizers and herbicides but also a larger impact of the macroclimate). They have a lower basal area

544 and lack the sharp increase in stem density towards the edge that is present in northern forests, which

545 helps buffering the forest from the exterior. Similarly, edge influences in drier forests could also be

546 underestimated. This means that in these forests, the spatial extent of edge influences of the adjacent

547 land might be more extended and larger buffer zones are required to protect the microclimate, forest

548 specialists and nutrient cycling in the forest interior. Since macroclimate variation over space

549 influences the forest edge structure in our study, climate change and more frequent extreme heat and

550 drought events (Meehl et al., 2007) might also impact the forest edge structure as predicted by higher

551 MAT and lower DMI-values.

552 Understanding the impact of the above-mentioned factors is important, even though one can hardly

553 control them. Via management and species composition, we can shape the forest edge structure to

554 buffer the interior. Considering species composition, we found a positive impact of shade tolerance

555 on PAI, FHD, canopy height and basal area and a negative impact on canopy openness. Selecting

556 more shade-tolerant species could thus improve the thermal buffering capacity of forests, as old-

557 growth forest characteristics (e.g. high canopy, biomass and complexity) are associated with a higher

558 macroclimatic buffering (Frey et al., 2016; Kovács et al., 2017). This is of vital importance in the era

559 of climate change (De Frenne et al., 2019). However, it is also known that mixing tree species with

560 complementary characteristics generates a dense and filled canopy (Pretzsch, 2014; Jucker et al.,

561 2015; Sercu et al., 2017). If we focus on management, thinning leads to canopy opening, a reduced

562 basal area, stem density and biomass and more abrupt gradients in biomass. These management

563 practices in turn, can increase the impact of edge influences from the adjacent land in the forest

564 interior. If we want to protect the forest interior, dense and gradual forest edges, on the other hand,

565 can be beneficial since they reduce both the magnitude and depth of edge influences (Harper et al.,

566 2005). Gradual edges are, for instance, less susceptible to atmospheric nitrogen deposition (Wuyts et

567 al., 2009) while a dense edge with a high canopy cover is important for the establishment of the forest

568 microclimate and the reduction of maximum temperatures (Zellweger et al., 2019a). On the other

569 hand, an increase in canopy openness, due to the harvest of trees, can locally increase the temperature

570 and the impact of macroclimate warming (Zellweger et al., 2019a).

571 We further show that the impact of management practices in the different regions is not static, but

572 influenced by the time since management (e.g. PAI increases from open to dense forests and edge-

573   to-interior gradients in PAI are modified by the management type). Such dynamics are at present

574   often ignored when studying microclimates or ecosystem functions such as carbon sequestration near

575   edges as most research focusses on static edges (Smith et al., 2018). Not taking into account such a

576   dynamic behaviour could, similarly to disregarding the large-scale variation in forest edge structure,

577   underestimate the impact of the buffering capacity of the forest interior.

578   *4.6 Implications for future research*

579   Even though we sampled in three management types and thereby a large variability in forest

580   complexity and openness, not the whole range of possible forest edge types was sampled. Therefore,

581   for instance, we lack natural and unmanaged edges, which are less abrupt but more complex (Esseen

582   et al., 2016). Extending the range of edge types in addition to a random selection of forest edges could

583   improve our insights on the impact of management on the forest edge structure. Further, since we

584   only investigated deciduous forests generally dominated by oaks, additional research on the impact

585   of macroclimate, management and distance to the forest edge in other forest types could render new

586   information. In coniferous forests, a more abrupt, less variable edge structure is to be expected as

587   their capacity to respond to gaps in the canopy or edge formation is limited in comparison to

588   deciduous trees (Esseen et al., 2016). Therefore, these edges probably receive a higher atmospheric

589   deposition and are less capable of buffering the impact of the macroclimate. Research by Renaud and

590   Rebetez (2009), for instance, already showed that buffering of maximum temperatures is linked to

591   canopy closure and therefore more pronounced in broadleaved and mixed forests than in forests

592   dominated by conifers.

593   The use of TLS in forest inventories is beneficial due to its objectivity and accuracy. Probably, the

594   most important advantage of TLS is the possibility to study metrics nearly impossible to quantify

595   with conventional forest inventory techniques (Dassot et al., 2011; Liang et al., 2016), such as the

596   vertical structural variability. However, this technique is still costly and especially time-consuming.

597   Even when using single-scan TLS, reducing the data acquisition time, the data processing remains

598   time-consuming. Conventional forestry techniques, on the other hand, are easy applicable and require

599 less data processing. Therefore, traditional methods to extract, for instance, stem density and basal

600 area do still have their advantages over TLS. A conventional forestry inventory can thus provide the

601 researcher with a profound basis on the forest structure, though if enhanced or very detailed forest

602 measurements are required (e.g. vertical variability), conventional techniques and TLS can be very

603 complementary.

5. **Conclusions**

We studied differences in forest edge structure and their predictors for deciduous oak-dominated forests, subject to different management types along a large latitudinal gradient (2300 km) covering various macroclimatic zones in Europe. Macroclimate, forest management, distance to the forest edge and tree species composition all affected the forest edge structure. We found that edge influence could currently be underestimated in forests at lower latitudes, with a high MAT or lower water availability. Additionally, forest management interventions could negatively affect the edge quality (i.e. lower canopy cover and stem density and a higher canopy openness). This tends to reduce the microclimate buffering capacity of the forest and makes the edge more susceptible to atmospheric depositions. In drier regions, on the other hand, there might be positive effects of an intensive management (i.e. higher canopy height and FHD in open forests). We also found an impact of species composition on the forest edge structure. Selecting species with a higher shade tolerance could further increase the buffering capacity of the edge. Results on edge influences and management guidelines on forest edge structure can thus not be extrapolated or generalised across Europe, since both management and location matter.

Further research should focus on other factors that we did not quantify, such as variation in topography, soil properties, nitrogen deposition or biotic interactions with herbivores, with a potential influence on the forest edge structure. If we want to reduce edge influences due to forest fragmentation, more research is necessary to understand this large-scale variability in forest edge structure, to come up with proper region- and context-specific management guidelines.

Acknowledgements

References

Aussenac, G., 2000. Interactions between forest stands and microclimate: Ecophysiological aspects and consequences for silviculture. Ann. For. Sci. 57, 287–301. https://doi.org/10.1051/forest:2000119

Bates, D., Mächler, M., Bolker, B., Walker, S., 2015. Fitting linear mixed-effects models using lme4. J. Stat. Softw. 67, 1–48. https://doi.org/10.18637/jss.v067.i01

Baudry, O., Charmetant, C., Collet, C., Ponette, Q., 2014. Estimating light climate in forest with the convex densiometer: operator effect, geometry and relation to diffuse light. Eur. J. For. Res. 133, 101–110. https://doi.org/10.1007/s10342-013-0746-6

Bohn, U., Neuhäusl, R., 2000. Karte der natürlichen Vegetation Europas, BfN Schriftenvertrieb im Landwirtschaftsverlag. Bundesamt für Naturschutz, Bonn.

Broadbent, E.N., Asner, G.P., Keller, M., Knapp, D.E., Oliveira, P.J.C., Silva, J.N., 2008. Forest fragmentation and edge effects from deforestation and selective logging in the Brazilian Amazon. Biol. Conserv. 141, 1745–1757. https://doi.org/10.1016/J.BIOCON.2008.04.024

Brus, D.J., Hengeveld, G.M., Walvoort, D.J.J., Goedhart, P.W., Heidema, A.H., Nabuurs, G.J., Gunia, K., 2012. Statistical mapping of tree species over Europe. Eur. J. For. Res. 131, 145–157. https://doi.org/10.1007/s10342-011-0513-5

Cadenasso, M.L., Pickett, S.T.A., Weathers, K.C., Jones, C.G., 2003. A framework for a theory of ecological boundaries. Bioscience 53, 750–758. https://doi.org/10.1641/0006-3568(2003)053[0750:affato]2.0.co;2

Calders, K., Armston, J., Newnham, G., Herold, M., Goodwin, N., 2014. Implications of sensor configuration and topography on vertical plant profiles derived from terrestrial LiDAR. Agric. For. Meteorol. 194, 104–117. https://doi.org/10.1016/J.AGRFORMET.2014.03.022

Canham, C.D., Finzi, A.C., Pacala, S.W., Burbank, D.H., 1994. Causes and consequences of resource heterogeneity in forests: interspecific variation in light transmission by canopy trees. Can. J. For. Res. 24, 337–349. https://doi.org/10.1139/x94-046

Chen, J., Saunders, S.C., Crow, T.R., Naiman, R.J., Brosofske, K.D., Mroz, G.D., Brookshire, B.L., Franklin, J.F., 1999. Microclimate in forest ecosystem and landscape ecology. Bioscience 49, 288–297.

659   https://doi.org/10.2307/1313612

660 Chen J., Franklin, J.F., Spies, T.A., 1995. Growing-season microclimatic gradients from clearcut edges into

661   old-growth Douglas-fir forests. Ecol. Appl. 5, 74–86. https://doi.org/10.2307/1942053

662 Correll, D.L., 1991. Human impact on the functioning of landscape boundaries, in: Holland., M.M., Risser.,

663   P.G., Naiman, R.J. (Eds.), Ecotones: The Role of Landscape Boundaries in the Management and

664   Restoration of Changing Environments. Springer US, Boston, MA, pp. 90–109.

665   https://doi.org/10.1007/978-1-4615-9686-8

666 Dassot, M., Constant, T., Fournier, M., 2011. The use of terrestrial LiDAR technology in forest science:

667   application fields, benefits and challenges. Ann. For. Sci. 68, 959–974. https://doi.org/10.1007/s13595-

668   011-0102-2

669 Davies-Colley, R.J., Payne, G.W., Van Elswijk, M., 2000. Microclimate gradients across a forest edge. N. Z.

670   J. Ecol. 24, 111–121.

671 De Frenne, P., Zellweger, F., Rodríguez-Sánchez, F., Scheffers, B.R., Hylander, K., Luoto, M., Vellend, M.,

672   Verheyen, K., Lenoir, J., 2019. Global buffering of temperatures under forest canopies. Nat. Ecol. Evol.

673   3, 744–749. https://doi.org/10.1038/s41559-019-0842-1

674 de Martonne, E., 1926. L'indice d'aridité. Bull. Assoc. Geogr. Fr. 3, 3–5.

675   https://doi.org/10.3406/bagf.1926.6321

676 De Schrijver, A., Devlaeminck, R., Mertens, J., Wuyts, K., Hermy, M., Verheyen, K., 2007. On the

677   importance of incorporating forest edge deposition for evaluating exceedance of critical pollutant loads.

678   Appl. Veg. Sci. 10, 293–298. https://doi.org/10.1111/j.1654-109X.2007.tb00529.x

679 Didham, R.K., Lawton, J.H., 1999. Edge structure determines the magnitude of changes in microclimate and

680   vegetation structure in tropical forest fragments. Biotropica 31, 17–30. https://doi.org/10.1111/j.1744-

681   7429.1999.tb00113.x

682 Ehbrecht, M., Schall, P., Ammer, C., Fischer, M., Seidel, D., 2019. Effects of structural heterogeneity on the

683   diurnal temperature range in temperate forest ecosystems. For. Ecol. Manage. 432, 860–867.

684   https://doi.org/10.1016/J.FORECO.2018.10.008

685   Esseen, P.-A., 1994. Tree mortality patterns after experimental fragmentation of an old-growth conifer forest.

686   Biol. Conserv. 68, 19–28. https://doi.org/10.1016/0006-3207(94)90542-8

687   Esseen, P.-A., Hedström Ringvall, A., Harper, K.A., Christensen, P., Svensson, J., 2016. Factors driving

688   structure of natural and anthropogenic forest edges from temperate to boreal ecosystems. J. Veg. Sci.

689   27, 482–492. https://doi.org/10.1111/jvs.12387

690   Ewers, R.M., Banks-Leite, C., 2013. Fragmentation impairs the microclimate buffering effect of tropical

691   forests. PLoS One 8, e58093. https://doi.org/10.1371/journal.pone.0058093

692   Frey, S.J.K., Hadley, A.S., Johnson, S.L., Schulze, M., Jones, J.A., Betts, M.G., 2016. Spatial models reveal

693   the microclimatic buffering capacity of old-growth forests. Sci. Adv. 2, e1501392.

694   https://doi.org/10.1126/sciadv.1501392

695   Ginn, S.E., Seiler, J.R., Cazell, B.H., Kreh, R.E., 1991. Physiological and growth responses of eight-year-old

696   loblolly pine stands to thinning. For. Sci. 37, 1030–1040.

697   https://doi.org/10.1093/forestscience/37.4.1030

698   Goetz, S., Steinberg, D., Dubayah, R., Blair, B., 2007. Laser remote sensing of canopy habitat heterogeneity

699   as a predictor of bird species richness in an eastern temperate forest, USA. Remote Sens. Environ. 108,

700   254–263. https://doi.org/10.1016/J.RSE.2006.11.016

701   Govaert, S., Meeussen, C., Vanneste, T., Bollmann, K., Brunet, J., Cousins, S.A.O., Diekmann, M., Graae,

702   B.J., Hedwall, P., Heinken, T., Iacopetti, G., Lenoir, J., Lindmo, S., Orczewska, A., Perring, M.P.,

703   Ponette, Q., Plue, J., Selvi, F., Spicher, F., Tolosano, M., Vermeir, P., Zellweger, F., Verheyen, K.,

704   Vangansbeke, P., De Frenne, P., 2019. Edge influence on understorey plant communities depends on

705   forest management. J. Veg. Sci. jvs.12844. https://doi.org/10.1111/jvs.12844

706   Greiser, C., Meineri, E., Luoto, M., Ehrlén, J., Hylander, K., 2018. Monthly microclimate models in a

707   managed boreal forest landscape. Agric. For. Meteorol. 250–251, 147–158.

708   https://doi.org/10.1016/J.AGRFORMET.2017.12.252

709   Grubb, P.J., 1998. A reassessment of the strategies of plants which cope with shortages of resources.

710   Perspect. Plant Ecol. Evol. Syst. 1, 3–31. https://doi.org/10.1078/1433-8319-00049

711 Haddad, N.M., Brudvig, L.A., Clobert, J., Davies, K.F., Gonzalez, A., Holt, R.D., Lovejoy, T.E., Sexton,

712 J.O., Austin, M.P., Collins, C.D., Cook, W.M., Damschen, E.I., Ewers, R.M., Foster, B.L., Jenkins,

713 C.N., King, A.J., Laurance, W.F., Levey, D.J., Margules, C.R., Melbourne, B.A., Nicholls, A.O.,

714 Orrock, J.L., Song, D.-X., Townshend, J.R., 2015. Habitat fragmentation and its lasting impact on

715 Earth's ecosystems. Sci. Adv. 1, e1500052. https://doi.org/10.1126/sciadv.1500052

716 Hamberg, L., Lehvävirta, S., Kotze, D.J., 2009. Forest edge structure as a shaping factor of understorey

717 vegetation in urban forests in Finland. For. Ecol. Manage. 257, 712–722.

718 https://doi.org/10.1016/J.FORECO.2008.10.003

719 Harper, K.A., Macdonald, S.E., Burton, P.J., Chen, J., Brosofske, K.D., Saunders, S.C., Euskirchen, E.S.,

720 Roberts, D., Jaiteh, M.S., Esseen, P.-A., 2005. Edge influence on forest structure and composition in

721 fragmented landscapes. Conserv. Biol. 19, 768–782. https://doi.org/10.1111/j.1523-1739.2005.00045.x

722 Harrington, C.A., Reukema, D.L., 1983. Initial shock and long-term stand development following thinning in

723 a Douglas-fir plantation. For. Sci. 29, 33–46.

724 Honnay, O., Verheyen, K., Hermy, M., 2002. Permeability of ancient forest edges for weedy plant species

725 invasion. For. Ecol. Manage. 161, 109–122. https://doi.org/10.1016/S0378-1127(01)00490-X

726 Hutchison, B.A., Matt, D.R., 1977. The distribution of solar radiation within a deciduous forest. Ecol.

727 Monogr. 47, 185–207. https://doi.org/10.2307/1942616

728 International Civil Aviation Organization., 1993. Manual of the ICAO standard atmosphere: extended to 80

729 kilometres (262 500 feet), 3rd ed. International Civil Aviation Organization, Montreal, Quebec.

730 Jennings, S., Brown, N., Sheil, D., 1999. Assessing forest canopies and understorey illumination: canopy

731 closure, canopy cover and other measures. Forestry 72, 59–74. https://doi.org/10.1093/forestry/72.1.59

732 Jucker, T., Bouriaud, O., Coomes, D.A., 2015. Crown plasticity enables trees to optimize canopy packing in

733 mixed-species forests. Funct. Ecol. 29, 1078–1086. https://doi.org/10.1111/1365-2435.12428

734 Karger, D.N., Conrad, O., Böhner, J., Kawohl, T., Kreft, H., Soria-Auza, R.W., Zimmermann, N.E., Linder,

735 H.P., Kessler, M., 2017. Climatologies at high resolution for the earth's land surface areas. Sci. Data 4,

736 170122. https://doi.org/10.1038/sdata.2017.122

737 Kleijn, D., Snoeijing, G.I.J., 1997. Field boundary vegetation and the effects of agrochemical drift: botanical

738   change caused by low levels of herbicide and fertilizer. J. Appl. Ecol. 34, 1413–1425.

739   https://doi.org/10.2307/2405258

740 Kuznetsova, A., Brockhoff, P.B., Christensen, R.H.B., 2017. lmerTest package: tests in linear mixed effects

741   models. J. Stat. Softw. 82, 1–26. https://doi.org/10.18637/jss.v082.i13

742 Laurance, W.F., Ferreira, L. V., Merona, J.M.R., Laurance, S.G., 1998. Rain forest fragmentation and the

743   dynamics of Amazon tree communities. Ecology 79, 2032–2040. https://doi.org/10.1890/0012-

744   9658(1998)079[2032:RFFATD]2.0.CO;2

745 Lenoir, J., Hattab, T., Pierre, G., 2017. Climatic microrefugia under anthropogenic climate change:

746   implications for species redistribution. Ecography. 40, 253–266. https://doi.org/10.1111/ecog.02788

747 Liang, X., Kankare, V., Hyyppä, J., Wang, Y., Kukko, A., Haggrén, H., Yu, X., Kaartinen, H., Jaakkola, A.,

748   Guan, F., Holopainen, M., Vastaranta, M., 2016. Terrestrial laser scanning in forest inventories. ISPRS

749   J. Photogramm. Remote Sens. 115, 63–77. https://doi.org/10.1016/J.ISPRSJPRS.2016.01.006

750 Lindenmayer, D.B., Margules, C.R., Botkin, D.B., 2000. Indicators of biodiversity for ecologically

751   sustainable forest management. Conserv. Biol. 14, 941–950. https://doi.org/10.1046/j.1523-

752   1739.2000.98533.x

753 MacArthur, R.H., MacArthur, J.W., 1961. On bird species diversity. Ecology 42, 594–598.

754   https://doi.org/10.2307/1932254

755 Magnago, L.F.S., Rocha, M.F., Meyer, L., Martins, S.V., Meira-Neto, J.A.A., 2015. Microclimatic

756   conditions at forest edges have significant impacts on vegetation structure in large Atlantic forest

757   fragments. Biodivers. Conserv. 24, 2305–2318. https://doi.org/10.1007/s10531-015-0961-1

758 Matlack, G.R., 1994. Vegetation dynamics of the forest edge - Trends in space and successional Time. J.

759   Ecol. 82, 113. https://doi.org/10.2307/2261391

760 McElhinny, C., Gibbons, P., Brack, C., Bauhus, J., 2005. Forest and woodland stand structural complexity:

761   Its definition and measurement. For. Ecol. Manage. 218, 1–24.

762   https://doi.org/10.1016/J.FORECO.2005.08.034

763   Meehl, G.A., Stocker, T.F., Collins, W.D., Friedlingstein, P., Gaye, T., Gregory, J.M., Kitoh, A., Knutti, R.,

764   Murphy, J.M., Noda, A., Raper, S.C.B., Watterson, I.G., Weaver, A.J., Zhao, Z.C., 2007. Global

765   climate projections, in: Solomon, S., Qin, D., Manning, M., Chen, Z., Marquis, M., Averyt, K.B.,

766   Tignor, M., Miller, H.L. (Eds.), Climate Change 2007: The Physical Science Basis. Cambridge

767   University Press, Cambridge, United Kingdom and New York, NY, USA, pp. 747–845.

768   Melin, M., Hinsley, S.A., Broughton, R.K., Bellamy, P., Hill, R.A., 2018. Living on the edge: utilising lidar

769   data to assess the importance of vegetation structure for avian diversity in fragmented woodlands and

770   their edges. Landsc. Ecol. 33, 895–910. https://doi.org/10.1007/s10980-018-0639-7

771   Mourelle, C., Kellman, M., Kwon, L., 2001. Light occlusion at forest edges: an analysis of tree architectural

772   characteristics. For. Ecol. Manage. 154, 179–192. https://doi.org/10.1016/S0378-1127(00)00624-1

773   Muir, J., Phinn, S., Eyre, T., Scarth, P., 2018. Measuring plot scale woodland structure using terrestrial laser

774   scanning. Remote Sens. Ecol. Conserv. 4, 320–338. https://doi.org/10.1002/rse2.82

775   Müller, J., Brandl, R., Brändle, M., Förster, B., de Araujo, B.C., Gossner, M.M., Ladas, A., Wagner, M.,

776   Maraun, M., Schall, P., Schmidt, S., Heurich, M., Thorn, S., Seibold, S., 2018. LiDAR-derived canopy

777   structure supports the more-individuals hypothesis for arthropod diversity in temperate forests. Oikos

778   127, 814–824. https://doi.org/10.1111/oik.04972

779   Niinemets, Ü., 2010. A review of light interception in plant stands from leaf to canopy in different plant

780   functional types and in species with varying shade tolerance. Ecol. Res. 25, 693–714.

781   https://doi.org/10.1007/s11284-010-0712-4

782   Niinemets, Ü., Valladares, F., 2006. Tolerance to shade, drought, and waterlogging of temperate northern

783   hemisphere trees and shrubs. Ecol. Monogr. 76, 521–547. https://doi.org/10.1890/0012-

784   9615(2006)076[0521:TTSDAW]2.0.CO;2

785   Palik, B.J., Murphy, P.G., 1990. Disturbance versus edge effects in sugar-maple/beech forest fragments. For.

786   Ecol. Manage. 32, 187–202. https://doi.org/10.1016/0378-1127(90)90170-G

787   Pike, N., 2011. Using false discovery rates for multiple comparisons in ecology and evolution. Methods

788   Ecol. Evol. 2, 278–282. https://doi.org/10.1111/j.2041-210X.2010.00061.x

789   Pretzsch, H., 2014. Canopy space filling and tree crown morphology in mixed-species stands compared with

790   monocultures. For. Ecol. Manage. 327, 251–264. https://doi.org/10.1016/J.FORECO.2014.04.027

791   Quesada, C.A., Phillips, O.L., Schwarz, M., Czimczik, C.I., Baker, T.R., Patiño, S., Fyllas, N.M., Hodnett,

792   M.G., Herrera, R., Almeida, S., Alvarez Dávila, E., Arneth, A., Arroyo, L., Chao, K.J., Dezzeo, N.,

793   Erwin, T., di Fiore, A., Higuchi, N., Honorio Coronado, E., Jimenez, E.M., Killeen, T., Lezama, A.T.,

794   Lloyd, G., López-González, G., Luizão, F.J., Malhi, Y., Monteagudo, A., Neill, D.A., Núñez Vargas,

795   P., Paiva, R., Peacock, J., Peñuela, M.C., Peña Cruz, A., Pitman, N., Priante Filho, N., Prieto, A.,

796   Ramírez, H., Rudas, A., Salomão, R., Santos, A.J.B., Schmerler, J., Silva, N., Silveira, M., Vásquez, R.,

797   Vieira, I., Terborgh, J., Lloyd, J., 2012. Basin-wide variations in Amazon forest structure and function

798   are mediated by both soils and climate. Biogeosciences 9, 2203–2246. https://doi.org/10.5194/bg-9-

799   2203-2012

800   R Core Team (2019). R: A language and environment for statistical computing. R Foundation

801   for Statistical Computing, Vienna, Austria. URL https://www.R-project.org/.

802   Remy, E., Wuyts, K., Boeckx, P., Ginzburg, S., Gundersen, P., Demey, A., Van Den Bulcke, J., Van Acker,

803   J., Verheyen, K., 2016. Strong gradients in nitrogen and carbon stocks at temperate forest edges. For.

804   Ecol. Manage. 376, 45–58. https://doi.org/10.1016/J.FORECO.2016.05.040

805   Renaud, V., Rebetez, M., 2009. Comparison between open-site and below-canopy climatic conditions in

806   Switzerland during the exceptionally hot summer of 2003. Agric. For. Meteorol. 149, 873–880.

807   https://doi.org/10.1016/j.agrformet.2008.11.006

808   Riitters, K., Wickham, J., Costanza, J.K., Vogt, P., 2016. A global evaluation of forest interior area dynamics

809   using tree cover data from 2000 to 2012. Landsc. Ecol. 31, 137–148. https://doi.org/10.1007/s10980-

810   015-0270-9

811   Saunders, S.C., Chen, J., Drummer, T.D., Crow, T.R., 1999. Modeling temperature gradients across edges

812   over time in a managed landscape. For. Ecol. Manage. 117, 17–31. https://doi.org/10.1016/S0378-

813   1127(98)00468-X

814   Schmidt, M., Jochheim, H., Kersebaum, K.-C., Lischeid, G., Nendel, C., 2017. Gradients of microclimate,

815   carbon and nitrogen in transition zones of fragmented landscapes – a review. Agric. For. Meteorol. 232,

816   659–671. https://doi.org/10.1016/J.AGRFORMET.2016.10.022

817   Schmidt, M., Lischeid, G., Nendel, C., 2019. Microclimate and matter dynamics in transition zones of forest

818   to arable land. Agric. For. Meteorol. 268, 1–10. https://doi.org/10.1016/J.AGRFORMET.2019.01.001

819   Seidel, D., Ehbrecht, M., Puettmann, K., 2016. Assessing different components of three-dimensional forest

820   structure with single-scan terrestrial laser scanning: A case study. For. Ecol. Manage. 381, 196–208.

821   https://doi.org/10.1016/J.FORECO.2016.09.036

822   Seidel, D., Fleck, S., Leuschner, C., Hammett, T., 2011. Review of ground-based methods to measure the

823   distribution of biomass in forest canopies. Ann. For. Sci. 68, 225–244. https://doi.org/10.1007/s13595-

824   011-0040-z

825   Sercu, B.K., Baeten, L., van Coillie, F., Martel, A., Lens, L., Verheyen, K., Bonte, D., 2017. How tree

826   species identity and diversity affect light transmittance to the understory in mature temperate forests.

827   Ecol. Evol. 7, 10861–10870. https://doi.org/10.1002/ece3.3528

828   Smith, I.A., Hutyra, L.R., Reinmann, A.B., Marrs, J.K., Thompson, J.R., 2018. Piecing together the

829   fragments: elucidating edge effects on forest carbon dynamics. Front. Ecol. Environ. 16, 213–221.

830   https://doi.org/10.1002/fee.1793

831   Stogsdili, W.R., Wittwer, R.F., Hennessey, T.C., Dougherty, P.M., 1992. Water use in thinned loblolly pine

832   plantations. For. Ecol. Manage. 50, 233–245. https://doi.org/10.1016/0378-1127(92)90338-A

833   Strayer, D.L., Power, M.E., Fagan, W.F., Pickett, S.T.A., Belnap, J., 2003. A classification of ecological

834   boundaries. Bioscience 53, 723–729. https://doi.org/10.1641/0006-3568(2003)053[0723:acoeb]2.0.co;2

835   Taubert, F., Fischer, R., Groeneveld, J., Lehmann, S., Müller, M.S., Rödig, E., Wiegand, T., Huth, A., 2018.

836   Global patterns of tropical forest fragmentation. Nature 554, 519–522.

837   https://doi.org/10.1038/nature25508

838   van Leeuwen, M., Nieuwenhuis, M., 2010. Retrieval of forest structural parameters using LiDAR remote

839   sensing. Eur. J. For. Res. 129, 749–770. https://doi.org/10.1007/s10342-010-0381-4

840   Wang, Q., Li, P., 2013. Canopy vertical heterogeneity plays a critical role in reflectance simulation. Agric.

841   For. Meteorol. 169, 111–121. https://doi.org/10.1016/J.AGRFORMET.2012.10.004

842   Watt, P.J., Donoghue, D.N.M., 2005. Measuring forest structure with terrestrial laser scanning. Int. J.

843   Remote Sens. 26, 1437–1446. https://doi.org/10.1080/01431160512331337961

844   Weathers, K.C., Cadenasso, M.L., Pickett, S.T.A., 2001. Forest edges as nutrient and pollutant concentrators:

845   potential synergisms between fragmentation, forest canopies, and the atmosphere. Conserv. Biol. 15,

846   1506–1514. https://doi.org/10.1046/j.1523-1739.2001.01090.x

847   Wermelinger, B., Flückiger, P.F., Obrist, M.K., Duelli, P., 2007. Horizontal and vertical distribution of

848   saproxylic beetles (Col., Buprestidae, Cerambycidae, Scolytinae) across sections of forest edges. J.

849   Appl. Entomol. 131, 104–114. https://doi.org/10.1111/j.1439-0418.2006.01128.x

850   Wilkes, P., Lau, A., Disney, M., Calders, K., Burt, A., Gonzalez de Tanago, J., Bartholomeus, H., Brede, B.,

851   Herold, M., 2017. Data acquisition considerations for Terrestrial Laser Scanning of forest plots.

852   Remote Sens. Environ. 196, 140–153. https://doi.org/10.1016/J.RSE.2017.04.030

853   Wuyts, K., De Schrijver, A., Vermeiren, F., Verheyen, K., 2009. Gradual forest edges can mitigate edge

854   effects on throughfall deposition if their size and shape are well considered. For. Ecol. Manage. 257,

855   679–687. https://doi.org/10.1016/J.FORECO.2008.09.045

856   Young, A., Mitchell, N., 1994. Microclimate and vegetation edge effects in a fragmented podocarp-broadleaf

857   forest in New Zealand. Biol. Conserv. 67, 63–72. https://doi.org/10.1016/0006-3207(94)90010-8

858   Zellweger, F., Coomes, D., Lenoir, J., Depauw, L., Maes, S.L., Wulf, M., Kirby, K.J., Brunet, J., Kopecký,

859   M., Máliš, F., Schmidt, W., Heinrichs, S., den Ouden, J., Jaroszewicz, B., Buyse, G., Spicher, F.,

860   Verheyen, K., De Frenne, P., 2019a. Seasonal drivers of understorey temperature buffering in

861   temperate deciduous forests across Europe. Glob. Ecol. Biogeogr. 28, 1774–1786.

862   https://doi.org/10.1111/geb.12991

863   Zellweger, F., De Frenne, P., Lenoir, J., Rocchini, D., Coomes, D., 2019b. Advances in microclimate

864   ecology arising from remote sensing. Trends Ecol. Evol. 34, 327–341.

865   https://doi.org/10.1016/j.tree.2018.12.012

866   Zellweger, F., Roth, T., Bugmann, H., Bollmann, K., 2017. Beta diversity of plants, birds and butterflies is

867   closely associated with climate and habitat structure. Glob. Ecol. Biogeogr. 26, 898–906.

868   https://doi.org/10.1111/geb.12598

869   Zuur, A., Ieno, E., Walker, N., Saveliev, A., Smith, G., 2009. Mixed effects modelling for nested data, in:

870   Zuur, A.F., Ieno, E.N., Walker, N.J., Saveliev, A.A., Smith, G.M. (Eds.), Mixed Effects Models and

871   Extensions in Ecology with R. Springer, New York, NY, USA, pp. 101–142.

872